



NIH Public Access

Author Manuscript

Brain Imaging Behav. Author manuscript; available in PMC 2014 February 18.

Published in final edited form as:

Brain Imaging Behav. 2011 September ; 5(3): 189–202. doi:10.1007/s11682-011-9123-6.

A few thoughts on brain ROIs

Tianming Liu

Department of Computer Science and Bioimaging Research Center, The University of Georgia, Athens, GA 30602, USA

Tianming Liu: tliu@cs.uga.edu

Abstract

Quantitative mapping of structural and functional connectivities in the human brain via non-invasive neuroimaging offers an exciting and unique opportunity to understand brain architecture. Because connectivity alterations are widely reported in a variety of brain diseases, assessment of structural and functional connectivities has emerged as a fundamental research area in clinical neuroscience. A fundamental question arises when attempting to map structural and functional connectivities: how to define and localize the best possible Regions of Interests (ROIs) for brain connectivity mapping? Essentially, when mapping brain connectivities, ROIs provide the structural substrates for measuring connectivities within individual brains and for pooling data across populations. Thus, identification of reliable, reproducible and accurate ROIs is critically important for the success of brain connectivity mapping. This paper discusses several major challenges in defining optimal brain ROIs from our perspective and presents a few thoughts on how to deal with those challenges based on recent research work done in our group.

Keywords

Region of interests; Diffusion tensor imaging; functional MRI; Brain connectivity

Introduction

Segregation and integration is a general principle of the brain's functional architecture (Friston 2009; Ashburner et al. 2004). It is widely believed that the brain's function is integrated via structural and functional connectivities (Biswal 2010; Sporns et al. 2005; Van Dijk et al. 2010; Hagmann et al. 2010; Friston et al. 2003). Therefore, analysis of brain connectivity is of significant importance to brain imaging and neuroscience (Biswal 2010; Sporns et al. 2005; Van Dijk et al. 2010; Hagmann et al. 2010; Friston et al. 2003; Bullmore and Sporns 2009). Essentially, when mapping brain connectivity, Regions of Interests (ROIs) provide the structural substrates for measuring connectivities within individual brains and for pooling data across populations. Identification of reliable, reproducible and accurate ROIs is critically important for the success of brain connectivity mapping. Therefore, a fundamental question arises when attempting to measure brain connectivities: how to define and localize the best possible ROIs? Current approaches for identifying ROIs in brain imaging can be broadly classified into four categories (Li et al. 2009a). The first is manual labeling by experts based on their domain knowledge (Sobel et al. 1993). While widely used, this method is vulnerable to inter-subject and intra-subject variation and its reproducibility may be low. The second method is to cluster ROIs from the brain image itself and is data-driven (Zang et al. 2004; Hyvärinen and Oja 2000; Beckmann et al. 2005;

Calhoun et al. 2004). However, these data-driven approaches are typically sensitive to the clustering parameters used, and their neuroscience interpretation is not clear. The third one is to predefine ROIs in a template brain, and warp them to the individual space using image registration algorithms (Shen and Davatzikos 2002). The accuracy of these atlas-based warping methods is limited due to the remarkable variability of neuroanatomy across different brains. The fourth method uses task-based fMRI paradigms to identify activated brain regions as ROIs. This methodology is regarded as the benchmark approach for ROI identification.

However, task-based fMRI itself has limitations, and is subject to a variety of variables that might affect the accuracy of detected ROIs (Jo et al. 2008; Geissler et al. 2005; White et al. 2001). For instance, a few recent studies (Jo et al. 2008; Geissler et al. 2005; White et al. 2001) reported that the locations of detected fMRI activations could be significantly shifted due to spatial smoothing, which is commonly used in popular fMRI analysis toolkits such as FSL (<http://fsl.fmrib.ox.ac.uk/fsl/feat5/>), SPM (<http://www.fil.ion.ucl.ac.uk/spm/>) and AFNI (<http://afni.nimh.nih.gov/afni>) in order to increase signal-to-noise ratio and facilitate aggregating data across subjects. As shown in Fig. 1a, because the local maximum of the ROI was shifted by 4 mm due to spatial smoothing (Li et al. 2010a), its structural profile (Fig. 1b) was significantly altered. In short, existing ROI identification approaches, including task-based fMRI, are inadequate to accurately localize ROIs (Li et al. 2010a).

Why identification of brain ROIs is so challenging?

So far, ROI identification is still an open, urgent problem in many brain imaging applications including brain connectivity mapping. From our perspective, the major challenges come from three critical reasons: 1) The boundaries between cortical regions are unclear (Van Essen and Dierker 2007; Handbook of Functional Neuroimaging of Cognition); 2) The individual variability of cortical anatomy, connection and function is remarkable (Brett et al. 2002); 3) The properties of ROIs are highly nonlinear. For instance, a slight change of the size or location of a ROI might dramatically alter its structural and functional connectivity profiles (Fig. 1b) (Li et al. 2010a).

Boundaries between cortical regions

In vivo parcellation of the cerebral cortex from brain imaging data has been extensively studied in the past two decades for definition of brain ROIs at the scale of gyral or sulcal regions. Current approaches to cortical parcellation can be broadly classified into two categories: model-driven or data-driven methods. In model-driven methods, the atlas-based warping method is widely used. For instance, the FreeSurfer system (Fischl et al. 1999) and the HAMMER algorithm (Shen et al. 2002) can be used to parcellate a subject's cortex by transforming an expert-labeled atlas to the subject's space. In data-driven approaches, people have used geometrical (Fischl et al. 1999; Shen et al. 2002; Li et al. 2009b), morphological (Van Essen and Dierker 2007), connectional (Behrens et al. 2003), or functional (Cohen et al. 2008) features to guide the parcellation procedure. An essential issue in cortical parcellation approaches is what features or attributes should be used to define the cortical region boundaries, no matter it is model-driven or data-driven. For instance, cortical geometric folding patterns might be good for sulcal or gyral parcellation (Li et al. 2009b, 2010d). Figure 2 demonstrates 6 examples of gyral parcellation via folding pattern based segmentation and atlas guided recognition (Li et al. 2010d). It is even possible to further parcellate a sulcus into finer-granularity sulcal banks (Li et al. 2010b) based on geometric shape features, as shown in Fig. 3.

However, it is unclear how the boundaries defined by geometric shape features, e.g., in Figs. 2 and 3, correlate with cytoarchitectural or functional boundaries. In addition, the brain

ROIs defined at the scale of gyral or sulcal regions might contain multiple functionally inhomogeneous subunits. Hence, definition of fine-granularity brain ROIs within functionally meaningful and homogeneous regions is much desired (Zhu et al. 2011). Recently, we attempted to develop a novel hybrid feature based on fiber shape and connectivity patterns for fine granularity gyrus parcellation (Zhu et al. 2011). The underlying premise is that each brain cytoarchitectonic area has a unique set of extrinsic inputs and outputs, called the ‘connectional fingerprint’ (Passingham et al. 2002), which is crucial in determining the function that each brain area performs (Passingham et al. 2002). We formulated the gyrus parcellation as a vertices clustering problem, as illustrated in Fig. 4. Both feature similarity and vertex adjacency are used to define the distance between vertices during the clustering (Passingham et al. 2002). Our results show that the precentral gyrus can be reasonably parcellated into 3 similar broad areas (Fig. 4i) on both hemispheres across different subjects, achieving finer granularity of regions than the traditional Brodmann areas. The parcellation results were partly verified via motor task-based fMRI studies (Fig. 4j) (Passingham et al. 2002).

However, it should be noted that the data-driven clustering approach in (Passingham et al. 2002) is still sensitive to the clustering parameters used. Though the affinity propagation clustering approach (Frey and Dueck 2007) we used in (Passingham et al. 2002) can automatically find the optimal cluster numbers and centers, it is still dependent on a few key parameters that need to be fine-tuned for specific dataset. For instance, there are many possibilities of clustering the similarity matrix in Fig. 4h into various numbers of cluster centers, resulting in different brain ROIs. In summary, it is an open question how to define the possible best boundaries in the cerebral cortex to optimally define brain ROIs.

Individual variability of cortical anatomy and function

The human cerebral cortex is a highly convoluted and complex anatomy composed of sulci and gyri. Evidence shows that cortical folding pattern can be described from multi-scale perspective (Li et al. 2010c). Curvature, as a very local descriptor of folding pattern, has been used to study the cortex folding patterns for its simple computation and effectiveness (Cachia et al. 2003). In addition, there are several meso-scale folding pattern descriptors that were developed recently. For example, we proposed a parametric representation of cortical folding patterns via polynomial models (Zhang et al. 2009). This parametric folding descriptor classifies meso-scale cortical surface patches into eight primitive patterns, including peak, pit, ridge, valley, saddle ridge, saddle valley, flat, and inflection. Recently, we proposed a gyrus-scale folding pattern analysis technique via cortical surface profiling (Li et al. 2010c). This approach combines advantages of a parametric method (achieving compact representation of shape) and a profiling method (achieving flexibility of arbitrary shape representation) and classify human gyral folding patterns into three classes according to their numbers of hinges: 2-hinge, 3-hinge and 4-hinge gyri. It has been demonstrated in the literature, including our own work (Li et al. 2010c; Zhang et al. 2009), that cortical folding patterns at the curvature, meso-scale and gyral-scale are very variable across individuals. Figure 5 depicts an example at the gyral scale. The remarkable variation of cortical anatomy raises significant challenges to identifying corresponding brain ROIs in different brains.

There are several folding descriptors of more global scale such as gyration index (GI) (Zilles et al. 1988) and overcomplete spherical wavelets (Yeo et al. 2008). The GI metric was used to compute the ratio between the pial contour and the outer contour in successive coronal sections, and already had a variety of applications. Recently, Toro et al. proposed surface ratio as a description extended from global scale, e.g., GI, to describe local cortical folding pattern (Toro et al. 2008). Also, the overcomplete spherical wavelets (Yeo et al.

2008), considering the trade-off between local and global scale representation of folding pattern, were used for shape analysis of cortical surface. Chung et al. employed a weighted linear combination of spherical harmonics for global representation of folded cortical surfaces (Chung et al. 2008). Duchesnay et al. used over 6,000 features to describe the global cortex folding pattern (Duchesnay et al. 2007). Those large numbers of feature parameters come from the various attributes of extracted sulci, including the pure shape descriptors (length, area and junction length), absolute position (sulcus extremities, sulcus center of mass coordinates, and midpoint between two neighboring sulci in the Talairach space), and the spatial relationship between neighboring sulci.

In general, sulcal fundi are believed to be one of the most reliable features of cortical folding, and sulcal fundi are believed to be associated with functional and cytoarchitectural boundaries of cortical regions (Welker 1990). Hence, the composition of a collection of sulcal fundi could be a good representation of global cortical anatomy. Recently, we extracted fourteen major sulcal fundi including the central sulcus, post-central sulcus, pre-central sulcus, superior temporal sulcus, superior frontal sulcus, inferior frontal sulcus and cingulate sulcus in each hemisphere, from 281 brain MRI images using the method proposed in (Li et al. 2010e). Figure 6a and b display all of the extracted sulcal fundi on a smoothed cortical surface. It is evident that the distributions and shapes of these major sulci fundi are remarkably variable across different individuals. For instance, the superior frontal sulcus and inferior frontal sulcus have the significant variability, which imposes significant challenges to brain ROI identification and correspondence establishment across individual subjects.

In addition to anatomic variation, functional localization of brain ROIs on the cerebral cortex in different brains is even more variable. As an example, Fig. 7 shows the distribution of 16 ROIs of the working memory network in the Montreal Neurologic Institute (MNI) atlas space. The ROIs including bilateral insula, superior frontal gyrus, precentral gyrus, paracingulate gyrus, inferior parietal lobule, and precuneus, and left medial frontal gyrus, right dorsolateral prefrontal cortex, left occipital pole, and right lateral occipital gyrus were obtained by the OSPAN task fMRI (Faraco et al. 2011). The widespread distributions of these ROIs suggest the remarkable variation of functional localizations in different brains.

Nonlinear properties of ROIs

Cortical ROIs exhibit highly nonlinear properties in terms of structural and functional connectivity profiles. For instance, a slight change to the location of an ROI might dramatically alter its structural and functional connectivity pattern. As shown in Fig. 8, when the ROI is moved from the green position to the red position (Fig. 8a), its structural fiber connection pattern derived from DTI tractography changes dramatically from that in Fig. 8b to the one in Fig. 8c. Here, the fibers derived from streamline tractography were projected onto the cortex using methods in (Zhang et al. 2010), since it is difficult for DTI tractography to enter the gray matter due to the low diffusion anisotropy. At the same time, the fMRI BOLD signal for this ROI also changes significantly, as shown by the green and red time-series signals in Fig. 8b and c. The remarkable nonlinearity demonstrated in Fig. 8 imposes significant challenge to ROI identification within and across subjects. For example, the altered functional BOLD signal of brain ROI will have significant influence on the measurement of functional connectivity between the ROI in consideration and other ROIs. Similarly, a slight change to the size of an ROI might also dramatically alter its structural and functional connectivity pattern, as the fibers emanating from the ROI and fMRI signals contained in the ROI will be changed as well.

A few thoughts on ROI identification

In responses to the above discussed challenges in brain ROI identification, we made some initial effort to optimize, model and predict functionally meaningful ROIs within and across individual brains. The general principle underlying our work is that the optimized or predicted ROIs should have similar structural and functional connection patterns within a group of subjects.

Optimization of brain ROIs via maximization of group-wise consistency

Despite the high anatomic variability across subjects, there is deep-rooted regularity of brain architecture on which we base the proposed approaches. First, across subjects, the functional ROIs should have similar anatomical locations, e.g., those in the MNI atlas space (please refer to Fig. 7b). Second, these ROIs should have similar structural connectivity profiles across subjects. In other words, fibers penetrating the same functional ROIs should have at least similar target regions across subjects (Fig. 9a). Last, individual networks identified by task-based paradigms, such as the working memory network we adapted as a test bed in our pilot study, should have similar functional connectivity patterns across subjects. The neuroscience bases of the above premises include: 1) structural and functional brain connectivity are closely related (Passingham et al. 2002; Honey et al. 2009); Hence, it is reasonable to put these three types of information in a joint analysis framework (Li et al. 2010a). 2) Extensive studies have already demonstrated the existence of a common structural and functional architecture of the human brain (Van Dijk et al. 2010), and it is reasonable to assume that the common brain networks have similar structural and functional connectivity patterns across individuals. Based on these premises, we optimize the locations and sizes of individual ROIs by jointly modeling anatomic profiles, and structural and functional connectivity patterns (Li et al. 2010a). The goal is to minimize the group-wise variance (or maximize group-wise consistency) of the jointly modeled profiles. Mathematically, we modeled the problem as an energy function, which was minimized via the simulated annealing (Li et al. 2010a).

As an example, we used the brain ROIs detected in a working memory task (Faraco et al. 2011) as a test bed, and Fig. 9 shows the white matter fiber connections derived from DTI (Fig. 9a) and ROI locations before and after the optimization (Fig. 9b). Figure 9a shows the fibers penetrating the right precuneus for eight subjects before (top panel) and after optimization (bottom panel). The ROI is highlighted in a red sphere for each subject. As we can see from the figure (please refer to the highlighted yellow arrows), after optimization, the third and sixth subjects have significantly improved consistency with the rest of the group. By visual inspection, most of the ROIs moved to more reasonable and consistent locations after the optimization. As an example, Fig. 9b depicts the location movements of the ROI in Fig. 9a for eight subjects. As we can see, the ROIs for these subjects share a similar anatomical landmark, which appears to be the tip of the upper bank of the parieto-occipital sulcus. If the initial ROI was not at this landmark, it moved to the landmark after the optimization, which was the case for subjects 1, 4 and 7. The results in Fig. 9 indicate the significant improvement of ROI locations achieved by the optimization procedure (Li et al. 2010a). Hence, this ROI optimization method can be used to remedy the fMRI activation peak shift due to spatial smoothing. In general, this ROI optimization offers a promising solution to the challenges of unclear boundaries between cortical regions, the individual variability of cortical anatomy and connection, and nonlinear ROI properties.

Interestingly, a major observation that can be made from our results in Fig. 9 and in (Li et al. 2010a) is that white matter fiber connection pattern could be a good predictor of functional ROI. That is, the white matter fiber connection patterns for the same functional landmark in

different brains after optimization are quite consistent (Fig. 9a). This is in agreement with the “connectional fingerprint” concept presented in (Passingham et al. 2002) and the widely accepted concept that brain connection and function are closely related.

Identification of ROIs by visual analytics

Effective visual representations and interactions provide the mechanism for allowing experts to see and understand large volumes of information at once. Through a graphic user interface (GUI) (Fig. 10), raw multimodal imaging data can be transformed into compact and descriptive representation that is appropriate for the analytical task and effectively conveys the most important content of the large, complex, and dynamic neuroimaging data. Specifically, we have designed and implemented an in-house software for the GUI, as shown in Fig. 10. Figure 10a visualizes a cortical surface, on which the working memory ROIs are overlaid. The red arrow highlights a blue ROI under interactive editing, e.g., drag-and-drop to change its location. The DTI-derived fibers connecting to the moving blue ROI and the changing network connectivity are being updated in real time in response to the ROI change, as shown in Fig. 10b. The representative fMRI signal within this ROI, e.g., the first component after a PCA transform on the signals, is being updated in Fig. 10c, and the ROI’s locations in sagittal, axial and coronal volumetric images are updated in Fig. 10d.

In a pilot study, we predicted a functional ROI (left occipital pole, highlighted by the yellow arrows in Fig. 11(c)) with the aim of finding similar structural connectivity profiles for the ROI across subjects. In essence, this is a ROI prediction process based on visual structural connectivity pattern matching. In Fig. 11, panel (a) shows the fiber tracts that penetrate the ROI for 15 subjects (obtained in (Li et al. 2010a)). As can be seen, these fiber tracts have similar shapes, revealing this ROI has strong consistency in structural profiles across subjects. That is the reason why we consider these shapes as prior knowledge of structural connectivity pattern for this ROI, which serves as the matching target in ROI editing and prediction. Panel (b) and (c) depict the ROI’s fiber tracts before and after interactive visual editing. The first and third images show the ROI location from different views. The second image shows the corresponding fiber tracts, and the fourth image shows the functional connectivity network. It is apparent that after interactive editing, the ROI of this subject has a much better match in shape with other subjects, suggesting that this visual analytics approach offers an effective solution to the challenges of the individual variability of cortical anatomy and nonlinear ROI properties.

ROI prediction

In the above sections, we used multimodal fMRI and DTI data for ROI identification and optimization. However, in many application scenarios, there is no task-based fMRI data available. For instance, it is challenging to conduct task-based fMRI studies for young children or elderly subjects such as Alzheimer’s disease patients. Instead, DTI scan typically needs around 10 min, is much less demanding, and is widely available. Therefore, we are strongly motivated to accurately estimate the locations of functional ROIs by learning and applying statistical prior models of ROIs. Specifically, based on the above optimized ROIs (Fig. 9) and DTI data, we constructed consistent white matter fiber models as the predictors of functional ROIs in the training stage. In the prediction stage, DTI data of an individual subject was aligned to the standard space first. Then, starting from the average location of warped ROIs from the training dataset, an energy function was designed to iteratively optimize the ROIs’ locations. This energy function consists of internal and external terms. The internal term was measured by ROI coordinate reconstruction error, which corresponds to the ROI coordinate PCA model component; while the external term was defined by the

Hausdorff metric of ROIs' fiber bundles, which corresponds to the fiber bundle template component.

As a pilot study, we applied the ROI prediction approach on the ADNI-2 DTI datasets (Jack et al. 2010). To visualize the consistency of fiber bundles of predicted ROIs, we showed the fibers emanating from three predicted ROIs and fibers emanating from benchmark ROIs for two randomly selected testing ADNI-2 subjects in Fig. 12. In addition, corresponding fiber bundles of three subjects randomly selected from the training dataset are shown in Fig. 12 for comparison. It is evident that the fiber bundles of the predicted ROIs are quite similar to those of the corresponding ROIs in the training dataset (the first to third columns in Fig. 12). We also performed ROI prediction on healthy subjects with coincident fMRI and DTI datasets. The activation peaks provided by task-based fMRI was used as benchmark data. On average, the prediction error for ROIs over 5 separate subjects is 3.8 mm.

Scales of brain ROIs

In many previous studies, e.g., in (Bullmore and Sporns 2009), structural brain networks were typically constructed in a single resolution, that is, the sizes and numbers of graph nodes were fixed for the same dataset. However, structural brain networks can be viewed and defined at multiple scales, e.g., at micro-, meso-, or macro- scales. For instance, in our recent studies in (Yuan et al. 2011), we applied our recently developed approach based on fiber density guided cortical parcellation (Zhang et al. 2010) on high resolution DTI dataset to construct multi-resolution structural brain networks, shown in Fig. 13 as an example. Then, we use state-of-the-art graph analysis algorithms in GraphCrunch (Milenkovic et al. 2008) to measure the global and local graph properties of the structural networks. It turns out that graph properties in different resolutions could be significantly different (Yuan et al. 2011). It is also conceivable that structural connectivity patterns in networks of different scales are very different. At current stage, it is unclear which resolution is the best one to represent structural connectivity pattern of the brain. Interestingly, in a recent study of axonal wiring of Drosophila brain (Chiang et al. 2010), it was reported that the local processing unit (LPU) has remarkable consistency and reliability across many different Drosophila brains. Thus, we postulate that group-wise consistency is one of the fundamental principles that should guide the definition of brain ROIs for measurement of brain connectivity, no matter it is at the micro-, meso-, or macro- scales. Actually, this principle has already been used in our ROI optimization method in Fig. 9. In addition, future exploration of other fundamental principles is warranted.

Dynamics of functional connectivities between brain ROIs

Functional connectivities between brain ROIs have been extensively studied via functional MRI (fMRI) in recent years. Currently, many approaches for analysis of functional connectivities on brain networks assume temporal stationarity, that is, functional connectivities are computed over the entire scan and used to characterize the strengths of connections across regions. However, accumulating literature, including our own recent studies (Lim et al. 2011; Hu et al. 2011), have shown that functional brain connectivity is under dynamic changes in different time scales. As an example shown in Fig. 14a and b, we measured the temporal correlation of fMRI time series of two ends of a DTI-derived fiber to define the functional connectivity (FC) between the voxels it connects. Then, the FC patterns of all the white matter fibers within the whole brain are concatenated into a feature vector (Fig. 14c) to represent the brain's state (Lim et al. 2011). It is evident that the FC patterns of individual fibers, as well as the whole-brain, changes dramatically along the time axis.

Neuroscience research suggests that the function of any cortical area is subject to top-down influences of attention, expectation, and perceptual task (Gilbert and Sigman 2007). For instance, dynamic interactions between connections from higher- to lower-order cortical areas and intrinsic cortical circuits mediate the moment-by-moment functional switching in brain. Even in resting state, the functional connectivity is still under dynamic changes within time scales of seconds to minutes (Lindquist et al. 2007). In the literature, there has been growing number of studies that tackled the problem of modeling the dynamics of brain states and functional connectivity [e.g., (Lim et al. 2011; Hu et al. 2011; Gilbert and Sigman 2007; Lindquist et al. 2007; Robinson et al. 2010; Gao and Yee 2003; Morgan et al. 2004; Chang and Glover 2010)]. Despite significant progress in the literature, it is still an open and challenging problem, in our view, due to at least two critical reasons. 1) FMRI blood-oxygenation level dependent (BOLD) signal is characterized by its nonlinearity, non-stationarity and composition of signal components at multiple time scales (Heeger and Ress 2002; Logothetis 2008; Buzski and Draguhn 2004), which imposes significant challenges to inferring meaningful information from it. 2) Functional brain dynamics is a system behavior, and its quantitative modeling entails mathematically sound and biologically meaningful approaches.

Discussions and concluding remarks

In this article, the working memory network was used as a test bed system. Multimodal fMRI and DTI data was used for the ROI optimization, modeling and prediction. In the future, we plan to further evaluate and validate our ROI optimization and prediction framework (Li et al. 2010a) based on multimodal data for other brain networks such as attention, language, motor, emotion and vision systems using independent datasets. We envision that our framework would be a general framework that is applicable to reveal the common architecture of the human brain, represented by consistent structural connectivity patterns across individuals. In a broader sense, the optimized and modeled dense map of brain ROIs derived from multiple multimodal DTI and fMRI datasets can be considered and used as the next-generation brain atlas, which will have much finer granularity and better functional homogeneity than the Brodmann brain atlas that has been used in the brain science field for over 100 years. Furthermore, advanced diffusion imaging techniques such as HARDI (Tuch et al. 1999) have the potential to significantly improve current spatial and angular resolutions of DTI data, and more extensive evaluation studies are warranted to elucidate the relationships between structural connectivity and brain function.

In addition, the optimized ROI map can be used as a general reference coordinate system for functional brain mapping via fMRI. Over the past two decades, fMRI has had an enormous impact on how we study the human brain. However, the current common practice is to report stereotaxic coordinates for brain activations, usually in relation to the Talairach or the Montreal Neurological Institute coordinate system (74% of over 9,400 fMRI studies (Derrfuss and Mar 2009)). The accuracy with which we can compare coordinates will depend greatly on the similarity of the images, atlases, and normalization techniques used. In particular, comparison of functional localization and brain function from different fMRI imaging studies has been complicated by reporting the stereotaxic coordinates. With the availability of a dense ROI map optimized and modeled in the future, it will become possible to report functional activities in fMRI in relation to the identified ROIs. Since the ROIs are consistent across different brains with intrinsically established correspondences, the comparison and pooling of results from different fMRI studies become much more effective and efficient.

Finally, the ROI map will have significant and wide applications in clinical neuroscience. In general, clinical diagnosis, therapy and followup of numerous brain diseases entail accurate

localization of brain ROIs, which has been an open problem for years due to the practical difficulty of acquiring task-based fMRI data for patients. Essentially, the ROI prediction framework presented in this paper provides a promising solution to this challenging problem by offering an effective and efficient approach to estimating the localizations of functionally meaningful ROIs based on widely available DTI data. It should be noted, however, that structural and functional connectivities in diseased brains might have already been altered during disease progression. In this case, application of our approaches on a specific group of patients using an adaptive strategy will be warranted.

Acknowledgments

T Liu was supported by the NIH Career Award (NIH EB 006878), NIH R01 HL087923-03S2 and The University of Georgia start-up research funding. The author would like to thank Gang Li, Kaiming Li, Dajiang Zhu, Tuo Zhang, Chulwoo Lim, and Jianfei Yang for providing some of the figures used in this paper.

References

- Ashburner J, Friston K, Penny W. Human brain function. Academic Press; 2004.
- Beckmann CF, DeLuca M, Devlin JT, Smith SM. Investigations into resting-state connectivity using independent component analysis. *Philosophical Transactions of the Royal Society of London Series B: Biological Sciences*. 2005; 360:1001–1013.
- Behrens TEJ, et al. Non-invasive mapping of connections between human thalamus and cortex using diffusion imaging. *Nature Neuroscience*. 2003; 6:750–757.
- Biswal BB. Toward discovery science of human brain function. *PNAS*. 2010; 107(10):4734–4739. [PubMed: 20176931]
- Brett M, Johnsrude IS, Owen AM. The problem of functional localization in the human brain. *Nature Reviews Neuroscience*. 2002; 3(3):243–249.
- Bullmore E, Sporns O. Complex brain networks: graph theoretical analysis of structural and functional systems. *Nature Neuroscience Reviews*. 2009; 186(10)
- Buzski G, Draguhn A. Neuronal oscillations in cortical networks. *Science*. 2004; 304(5679):1926–1929. [PubMed: 15218136]
- Cachia A, Mangin JF, Rivière D, Kherif F, Boddaert N, Andrade A, et al. A primal sketch of the cortex mean curvature: a morphogenesis based approach to study the variability of the folding patterns. *IEEE Transactions on Medical Imaging*. 2003; 22:754–765. [PubMed: 12872951]
- Calhoun VD, Pekar JJ, Pearlson GD. Alcohol intoxication effects on simulated driving: exploring alcohol-dose effects on brain activation using functional MRI. *Neuropsychopharmacology*. 2004; 29:2097–3017. [PubMed: 15316570]
- Chang C, Glover GH. Time—frequency dynamics of resting-state brain connectivity measured with fMRI. *Neuroimage*. 2010; 50(1):81–98. [PubMed: 20006716]
- Chiang A, et al. Three-dimensional reconstruction of brain-wide wiring networks in drosophila at single-cell resolution. *Current Biology*. 2010; 21(1):1–11. [PubMed: 21129968]
- Chung M, Hartley R, Dalton K, Davidson R. Encoding cortical surface by spherical harmonics. *Statistica Sinica*. 2008; 18:1269–1291.
- Cohen AL, et al. Defining functional areas in individual human brains using resting functional connectivity MRI. *Neuroimage*. 2008; 41(1):45–57. [PubMed: 18367410]
- Derrfuss J, Mar RA. Lost in localization: the need for a universal coordinate database. *Neuroimage*. 2009
- Duchesnay E, Cachia A, Roche A, Rivière D, Cointepas Y, Papadopoulos-Orfanos D, et al. Classification based on cortical folding patterns. *IEEE Transactions on Medical Imaging*. 2007; 26(4):553–565. [PubMed: 17427742]
- Faraco CC, Unsworth N, Lagnely J, Terry D, Li K, Zhang D, et al. Complex span tasks offer a unique view of working and long term memory. *NeuroImage*. 2011
- Fischl B, et al. Cortical surface-based analysis II: inflation, flattening, and a surface-based coordinate system. *Neuroimage*. 1999; 9:195–207. [PubMed: 9931269]

- Frey BJ, Dueck D. Clustering by passing messages between data points. *Science*. 2007; 315:972–976. [PubMed: 17218491]
- Friston KJ. Modalities, modes, and models in functional neuroimaging. *Science*. 2009; 326(5951): 399–403. [PubMed: 19833961]
- Friston KJ, et al. Dynamic causal modeling. *Neuroimage*. 2003; 19:1273–1302. [PubMed: 12948688]
- Gao JH, Yee SH. Iterative temporal clustering analysis for the detection of multiple response peaks in fMRI. *Magnetic Resonance Imaging*. 2003; 21(1):51–53. [PubMed: 12620546]
- Geissler A, Lanzenberger R, Barth M, Tahamtan AR, Milakara D, Gartus A, et al. Influence of fMRI smoothing procedures on replicability of fine scale motor localization. *Neuroimage*. 2005; 24:323–331. [PubMed: 15627575]
- Gilbert CD, Sigman M. Brain states: top-down influences in sensory processing. *Neuron*. 2007; 54(5): 677–696. [PubMed: 17553419]
- Hagmann P, et al. MR connectomics: principles and challenges. *Journal of Neuroscience Methods*. 2010 Jan 22.
- Cabeza, Roberto; Kingstone, Alan. *Handbook of Functional Neuroimaging of Cognition*. 2.
- Heeger DJ, Ress D. What does fmri tell us about neuronal activity? *Nature Reviews Neuroscience*. 2002; 3(2):142–151.
- Honey CJ, et al. Predicting human resting-state functional connectivity from structural connectivity. *PNAS*. 2009; 106(6):2035–2040. [PubMed: 19188601]
- Hu X, et al. Assessing the dynamics on functional brain networks using spectral graph theory. *ISBI*. 2011; 2011
- Hyvärinen A, Oja E. Independent component analysis: algorithms and applications. *Neural Networks*. 2000; 13(4–5):411–430. [PubMed: 10946390]
- Jack CR Jr, Bernstein MA, Borowski BJ, Gunter JL, Fox NC, Thompson PM, et al. Update on the magnetic resonance imaging core of the Alzheimer's disease neuroimaging initiative. *Alzheimer's & Dementia*. 2010; 6(3):212–220.
- Jo HJ, Lee JM, Kim JH, Choi CH, Gu BM, Kang DH, et al. Artificial shifting of fMRI activation localized by volume-and surface-based analyses. *Neuroimage*. 2008; 40(3):1077–1089. [PubMed: 18291680]
- Li K, et al. Review of methods for functional brain connectivity detection using fMRI. *Computerized Medical Imaging and Graphics*. 2009a; 33(2):131–139. [PubMed: 19111443]
- Li G, et al. Automatic cortical sulcal parcellation based on surface principal direction flow field tracking. *Neuroimage*. 2009b; 46(4):923–937. [PubMed: 19328234]
- Li K, et al. Individualized ROI optimization via maximization of group-wise consistency of structural and functional profiles. *Advances in Neural Information Processing Systems (NIPS)*. 2010a
- Li G, et al. Cortical Sulcal Bank segmentation via graph partition: methods and applications. *MIAR (Medical Imaging and Augmented Reality)*. 2010b
- Li K, Guo L, Li G, Nie J, Faraco C, Cui G, et al. Gyral folding pattern analysis via surface profiling. *NeuroImage*. 2010c
- Li G, Guo L, Zhang T, Nie J, Liu T. Automatic cortical gyral parcellation using cortical probabilistic atlas and graph cuts. *MIAR (Medical Imaging and Augmented Reality)*. 2010d
- Li G, Guo L, Nie N, Liu T. An automated pipeline for sulci fundi extraction. *Medical Image Analysis*. 2010e; 14(3):343–359. [PubMed: 20219410]
- Lim C, Li X, Li K, Guo L, Liu T. Brain state change detection via fiber-centered functional connectivity analysis. *ISBI*. 2011; 2011
- Lindquist MA, Waugh C, Wager TD. Modeling state-related fMRI activity using change-point theory. *Neuroimage*. 2007; 35(3):1125–1141. [PubMed: 17360198]
- Logothetis NK. What we can do and what we cannot do with fmri. *Nature*. 2008; 453(7197):869–878. [PubMed: 18548064]
- Milenkovic T, et al. GraphCrunch: a tool for large network analyses. *BMC Bioinformatics*. 2008; 9:70. [PubMed: 18230190]

- Morgan VL, Price RR, Arain A, et al. Resting functional MRI with temporal clustering analysis for localization of epileptic activity without EEG. *Neuroimage*. 2004; 21(1):473–481. [PubMed: 14741685]
- Passingham RE, et al. The anatomical basis of functional localization in the cortex. *Nature Reviews Neuroscience*. 2002; 3(8):606–616.
- Robinson LF, Wager TD, Lindquist MA. Change point estimation in multi-subject fMRI studies. *Neuroimage*. 2010; 49(2):1581–1592. [PubMed: 19733671]
- Shen D, Davatzikos C. HAMMER: hierarchical attribute matching mechanism for elastic registration. *IEEE Transactions on Medical Imaging*. 2002; 21(11):1421–1439. [PubMed: 12575879]
- Shen D, et al. HAMMER: Hierarchical Attribute Matching Mechanism for Elastic Registration. *IEEE Transactions on Medical Imaging*. 2002; 21(11):1421–1439. [PubMed: 12575879]
- Sobel DF, Gallen CC, Schwartz BJ, Waltz TA, Copeland B, Yamada S, et al. Locating the central sulcus: comparison of MR anatomic and magnetoencephalographic functional methods. *AJR American Journal of Neuroradiology*. 1993; 14(4):915–925. [PubMed: 8352165]
- Sporns O, Tononi G, Kötter R. The human connectome: a structural description of the human brain. *PLoS Computational Biology*. 2005; 1(4):e42. [PubMed: 16201007]
- Toro R, Perron M, Pike B, Richer L, Veillette S, Pausova Z, et al. Brain size and folding of the human cerebral cortex. *Cerebral Cortex*. 2008; 18(10):2352–2357. [PubMed: 18267953]
- Tuch, DS., et al. ISMRM'1999. 1999. High angular resolution diffusion imaging of the human brain.
- Van Dijk KR, Hedden T, Venkataraman A, Evans KC, Lazar SW, Buckner RL. Intrinsic functional connectivity as a tool for human connectomics: theory, properties, and optimization. *Journal of Neurophysiology*. 2010; 103(1):297–321. [PubMed: 19889849]
- Van Essen DC, Dierker DL. Surface-based and probabilistic atlases of primate cerebral cortex. *Neuron*. 2007; 56
- Welker W. Why does cerebral cortex fissure and fold? A review of determinants of gyri and sulci. *Cerebral Cortex*. 1990; 8b
- White TO, Leary D, Magnotta V, Arndt S, Flaum M, Andreasen NC. Anatomic and functional variability: the effects of filter size in group fMRI data analysis. *Neuroimage*. 2001; 13:577–588. [PubMed: 11305887]
- Yeo BT, Yu P, Grant PE, Fischl B, Golland P. Shape analysis with overcomplete spherical wavelets. *Proc MICCAI, LNCS*. 2008; 5241:468–476.
- Yuan Y, et al. Assessing graph models for description of brain networks. *ISBI*. 2011; 2011
- Zang Y, et al. Regional homogeneity approach to fMRI data analysis. *Neuroimage*. 2004; 22(1):394–400. [PubMed: 15110032]
- Zhang, T.; Guo, L.; Li, G.; Nie, J.; Liu, T. Medical Image Computing and Computer Assisted Intervention (MICCAI). 2009. Parametric representation of cortical surface folding via polynomials.
- Zhang D, et al. Automatic cortical surface parcellation based on fiber density information. *International Symposium of Biomedical Imaging (ISBI)*. 2010; 2010
- Zhu D, et al. Fine granularity parcellation of Gyrus via fiber shape and connectivity based features. *ISBI*. 2011; 2011
- Zilles K, Armstrong E, Schleicher A, Kretschmann HJ. The human pattern of gyration in the cerebral cortex. *Anatomy and Embryology (Berl)*. 1988; 179:173–179.

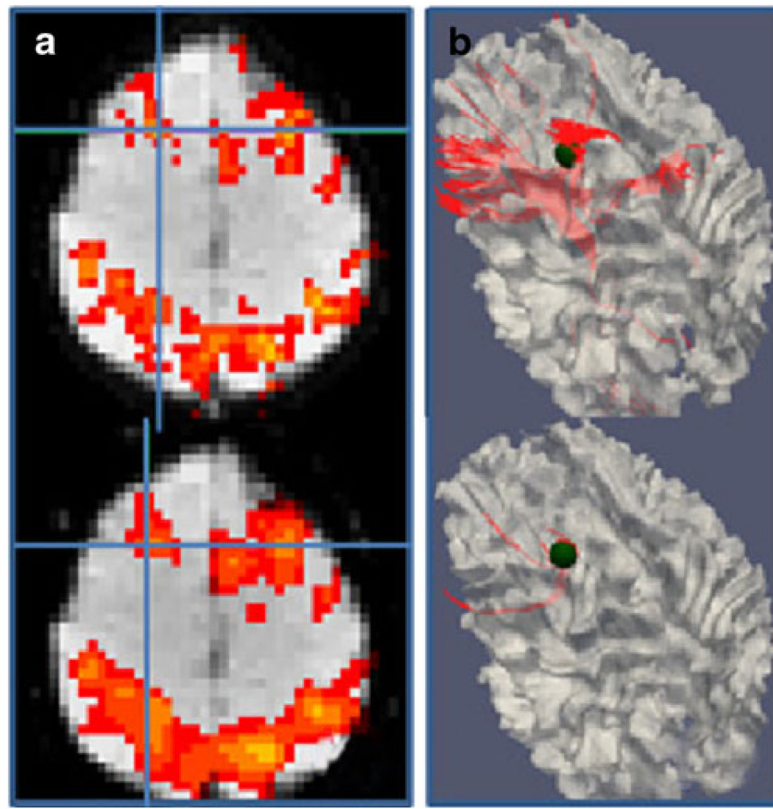


Fig. 1.

a Local activation map maxima (*marked by the cross*) shift of one ROI due to spatial volumetric smoothing in a working memory task (Faraco et al. 2011). The top one was detected using unsmoothed data while the bottom one used smoothed data (FWHM: 6.87 mm). **b** The corresponding fibers for the ROIs in (a). The ROIs are presented using a sphere (radius: 5 mm)

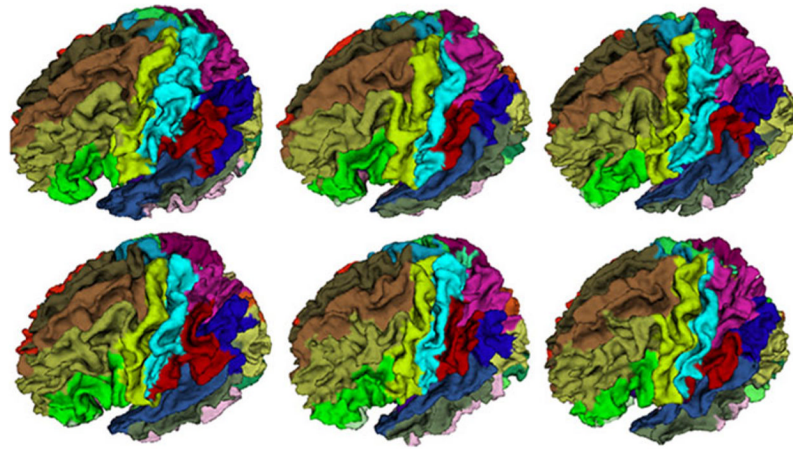


Fig. 2.

The gyral basin segmentation results by our hybrid method in (Li et al. 2010d) on the 6 cortical surfaces

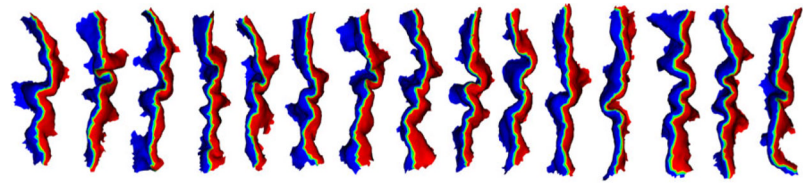
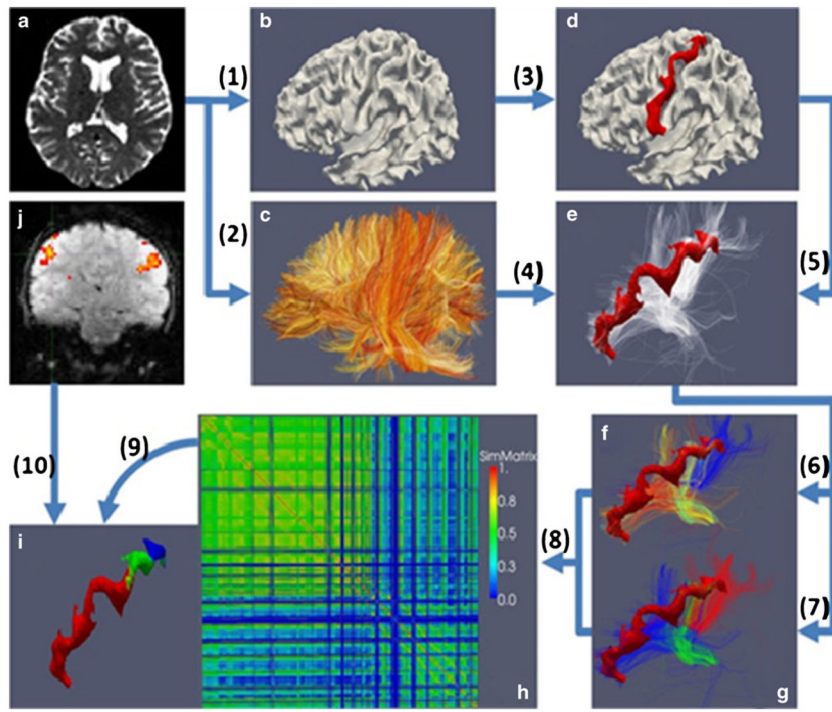


Fig. 3.

The sulcal bank segmentation results on 15 randomly selected central sulci (Li et al. 2010b). The central sulcal basins were segmented into anterior and posterior sulcal banks via geometric similarity based graph partition (Li et al. 2010b)

**Fig. 4.**

Flowchart of our methods. **a** DTI data; **b** Reconstructed cortical surface; **c** tracked fibers; **d** extracted precentral gyrus; **e** extracted fibers connecting precentral gyrus; **f** fiber shape patterns; **g** fiber connectivity patterns; **h** vertices similarity matrix; **i** gyrus parcellation result; **j** fMRI activation maps. (1): surface reconstruction; (2): fiber tracking; (3): cortical parcellation and gyrus extraction; (4)–(5): fiber extraction; (6): shape pattern clustering; (7) connectivity pattern clustering; (8): similarity matrix clustering using affinity propagation; (9): final segmentation result; (10): validation via fMRI

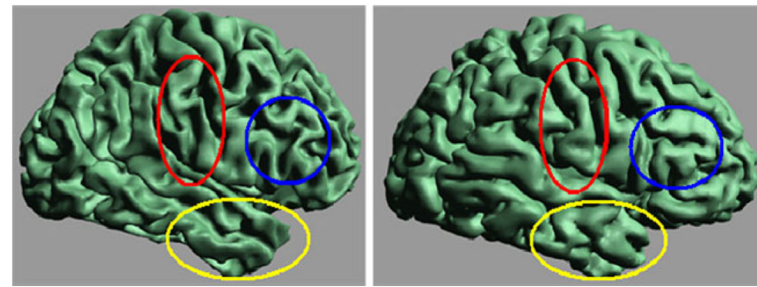


Fig. 5.

Illustration of different cortical folding patterns in two randomly selected human brains.
Each color represents a roughly corresponding cortical region

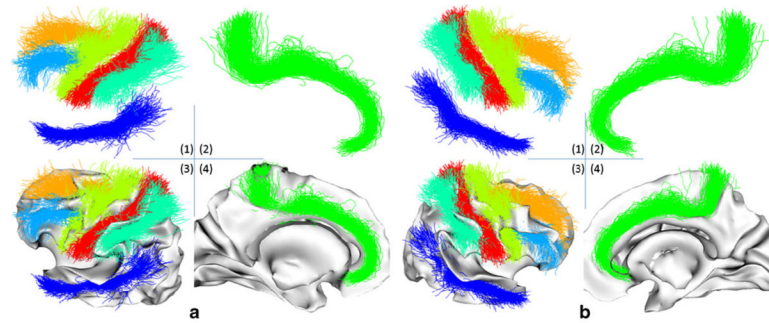


Fig. 6.

a–b All the extracted 14 sulcal fundi for the 281 subjects. **a** Sulcal fundi extracted from left hemispheres: 7 major sulcal fundi are shown in different colors (1, 2), and overlaid on a smoothed cortical surface (3, 4); **b** Sulcal fundi extracted from right hemispheres

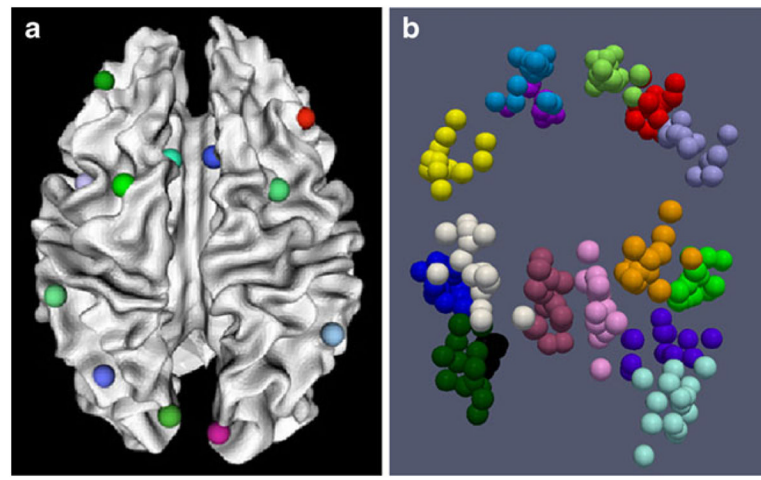


Fig. 7.

a ROI distribution in one subject. **b** ROI distributions of 15 subjects in the atlas space. Each ROI is represented by a sphere and different colors refer to different functional ROIs. 15 subjects were randomly selected and displayed. It is noted that the ROIs' colors in (a) do not correspond to those in (b)

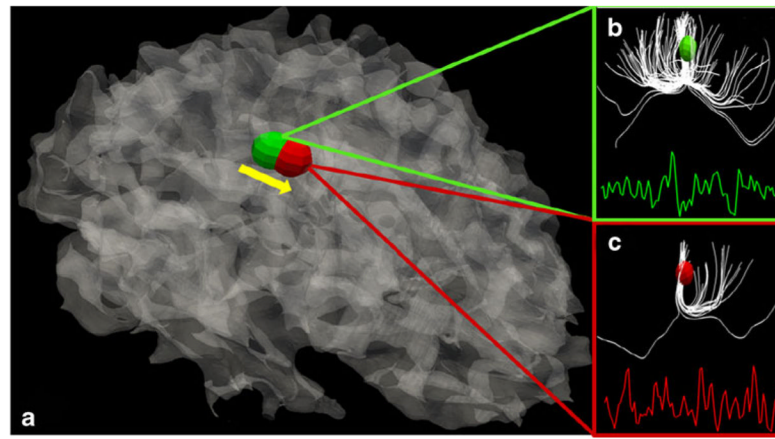


Fig. 8.

Illustration of structural and functional connectivity changes when the location of an ROI is changed slightly. **a** ROI location moves from the green to the red bubble. **b** Structural and functional (fMRI BOLD signal) profiles before the movement. **c** Structural and functional profiles after the movement

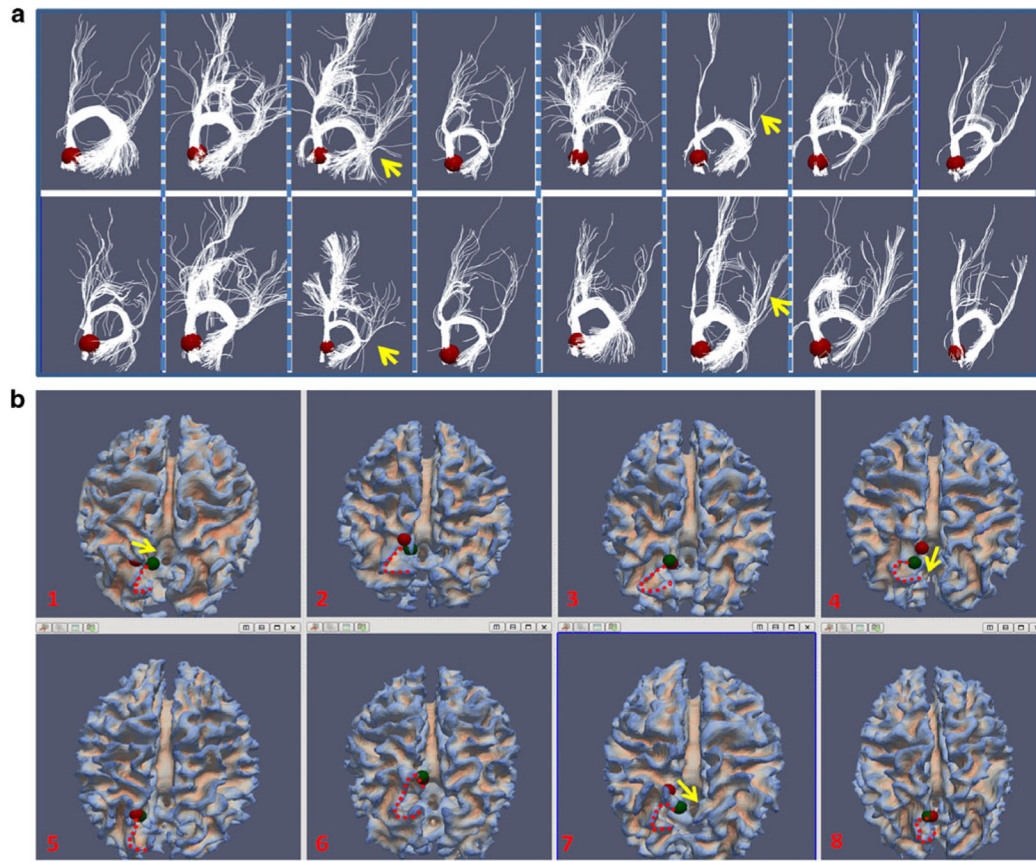


Fig. 9.

a Comparison of structural connection profiles before and after optimization. Each column shows the corresponding before-optimization (*top*) and after-optimization (*bottom*) fibers of one subject. The landmark (right precuneus) is presented by the red sphere. **b** The movement of right precuneus before (*in red sphere*) and after (*in green sphere*) optimization for eight subjects. The “C”-shaped red dash curve for each subject depicts a similar anatomical landmark across these subjects. The yellow arrows in subject 1, 4 and 7 visualize the movement direction after optimization

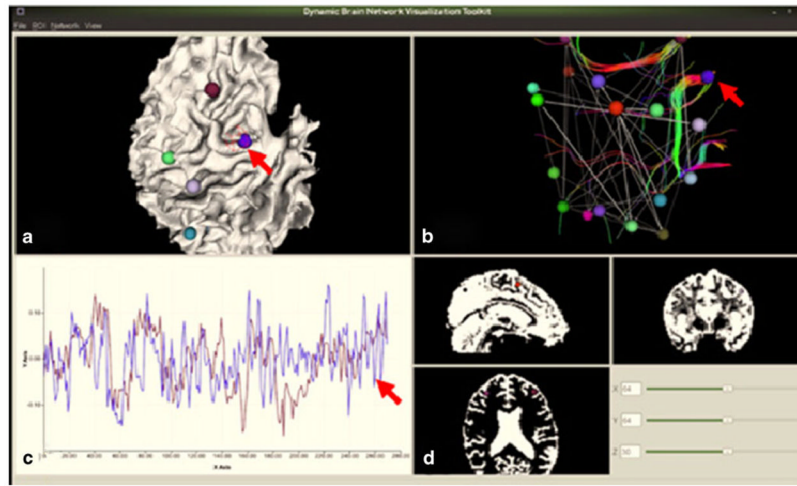


Fig. 10.

The GUI. **a** the view of cortical surface and ROIs; **b** the view of fibers and network; **c** fMRI signal view; **d** volume view

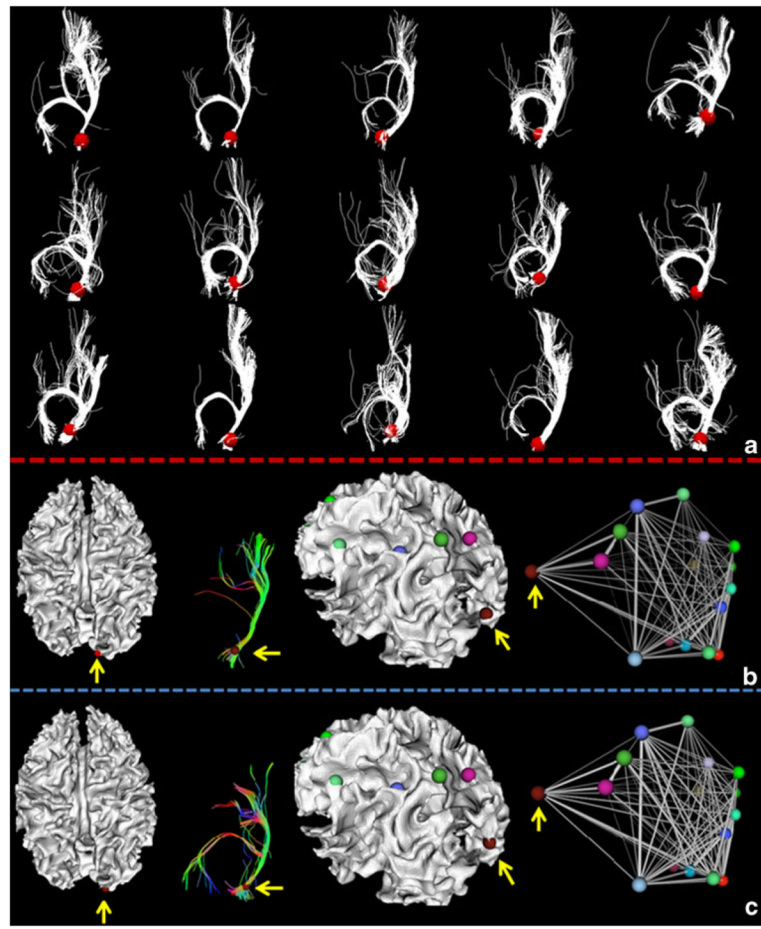


Fig. 11.

Interactive ROI prediction by using fiber profile as prior knowledge. **a** left occipital pole ROIs (*highlighted in dark red*) from 15 subjects with fiber tracts overlaid. **b** and **c** show the comparison before (**b**) and after (**c**) user interaction. The ROI is highlighted by yellow arrows. In each panel, the first image and third image show the ROI location from different views. The second image shows the corresponding fiber tracts, and the fourth image shows the functional connectivity network

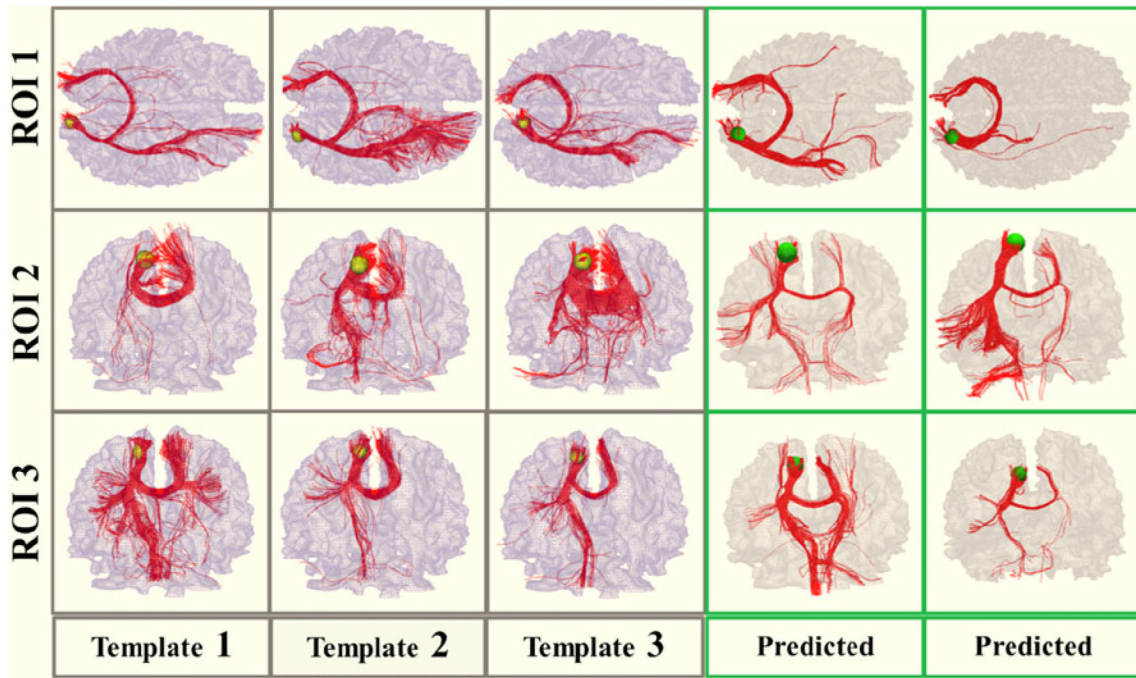


Fig. 12.

Visualization of fiber bundles of three predicted ROIs in MCI patients (Jack et al. 2010). Left gray frames: the template fiber bundles emanating from corresponding ROIs in the training dataset (*yellow bubbles*); Right green frames: fiber bundles emanating from predicted ROIs (*green bubbles*) in MCI patients

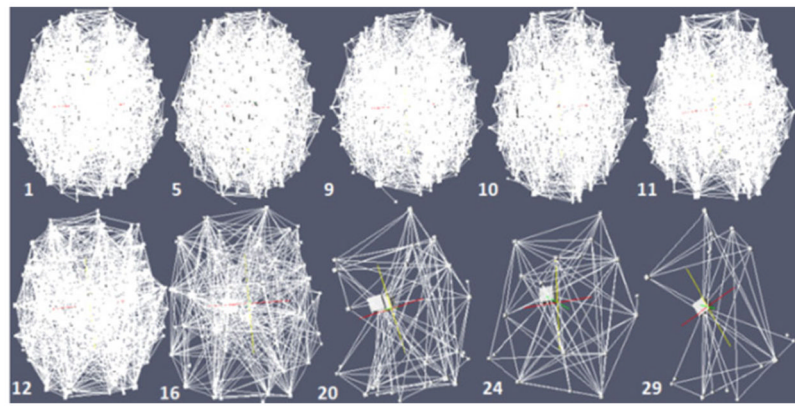


Fig. 13.

Examples of multi-resolution structural brain networks. 10 resolutions were illustrated for one subject. The number of nodes in each network is 2063, 2051, 1802, 1667, 1495, 1221, 447, 82, 38 and 21, respectively

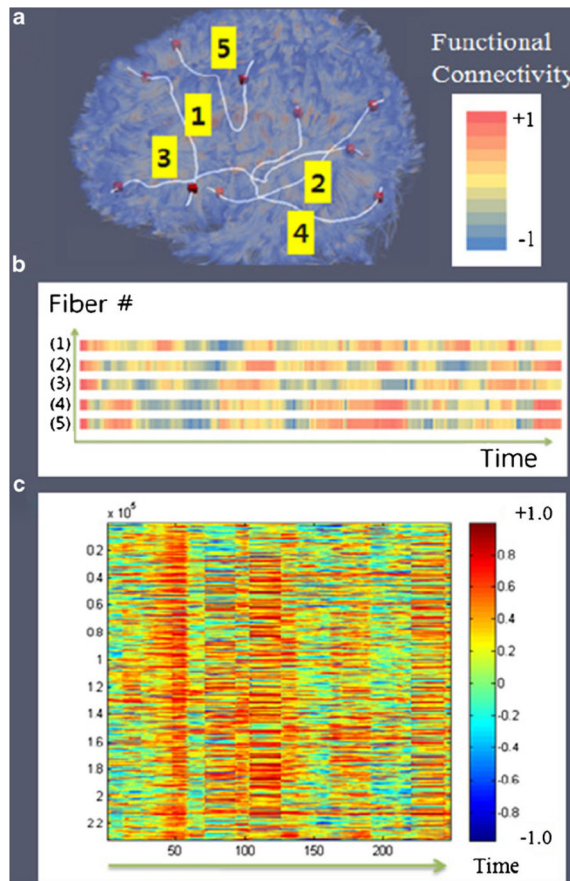


Fig. 14.

a DTI-derived fibers. Five fibers are highlighted and numbered. **b** Dynamic functional connectivities (DFCs) of five pairs of fiber end points along the time axis (seconds). Each row represents the DFC curve of a fiber in (a). The FC range is -1.0 to 1.0 . Color bar is on the top right. **c** DFC curves of all fibers in a brain are represented by the CSVs (columns) along the horizontal time axis